SLAC-PUB-7773
March 1998

QUANTUM EFFECTS IN TRACKING*

S. Heifets, Y.T. Yan

Stanford Linear Accelerator Center, Stanford University, Stanford, CA 94309, USA

Abstract

Quantum corrections to beam dynamics are considered. It is shown that quantum corrections included in tracking can substantially affect beam trajectory in the vicinity of the separatrix.

Contributed to Advanced ICFA Beam Dynamics Workshop on the Quantum Aspects of beam Physics, 1/4/98—1/9/98, Monterey, CA, USA

*Supported by Department of Energy contract DE-AC03-76SF00515.

QUANTUM EFFECTS IN TRACKING†

S. Heifets, Y.T. Yan

Stanford Linear Accelerator Center
Stanford University, Stanford, CA 94309, USA
E-mail: Heifets@slac.stanford.edu, E-mail: Yan@slac.stanford.edu

Abstract

Quantum corrections to beam dynamics are considered. It is shown that quantum corrections included in tracking can substantially affect beam trajectory in the vicinity of the separatrix.

1 Introduction

Quantum effects are usually disregarded in the study of beam stability. Indeed, Planck's constant h (divided by 2π) sets the limit $h/2$ on the minimum area of the phase space occupied by a particle. This limit may be compared with $p_0\epsilon$ where p_0 is the beam momentum, $p_0 = E/c$, and ϵ is the beam emittance defined as the product of the beam transverse rms $\epsilon = \Delta x \Delta x'$. For 1 GeV beam, this sets the limit $\epsilon > 10^{-16}$ m, much smaller than the typical 10^{-9} m in modern accelerators.

Bunches of electrons can be considered as an electron gas which can become degenerate at very large number of particles N_b per bunch. Again, this limit, $N_b\epsilon^3 \simeq> (h/2)^3$, is too far away from the limit $N_b \simeq 10^{10} - 10^{13}$ achievable today.

There is, however, a quantum effect which may become noticeable. We want to show that stochastic trajectories may be sensitive to quantum corrections. The reason for this is the exponential divergence of classical trajectories in stochastic areas.

The standard way of studying the stability of a particle in accelerators is tracking. This implies a description of particle motion in nonlinear but constant-in-time external fields with a map. The map is obtained from a Hamiltonian $H(x,p,t) = H_0 + V$, where the linear part, $H_0 = p^2/2 + \omega^2x^2/2$, describes betatron oscillations, and the perturbation V gives nonlinear but localized periodic kicks due to the nonlinear components of the magnetic system of an accelerator. Consider, for simplicity, the motion of a particle in the horizontal plane of a machine where, in addition to linear components providing

†Supported by Department of Energy contract DE–AC03–76SF00515.

focusing, there is only one thin octupole magnet which can be described by $V(x,t) = V_0(x)\delta_T(t)$, where $V_0(x) = \lambda(x^4/4)$ and $\delta_T(t)$ is the periodic delta-function with the revolution period T, $\delta_T(t+T) = \delta_T(t)$. The map then is the linear rotation from the coordinates (x,p) right after the octupole to the coordinates (x',p'), given by

$$\begin{aligned} x' &= x\cos\phi + (p/\omega)\sin\phi. \\ (p'/\omega) &= -x\sin\phi + (p/\omega)\cos\phi, \end{aligned} \tag{1}$$

right in front of the octupole after one turn, followed by the nonlinear octupole kick given by

$$\begin{aligned} \bar{x} &= x', \\ \bar{p} &= \lambda(x')^3, \end{aligned} \tag{2}$$

where $\phi = \omega T$. The map $(x,p) \rightarrow (\bar{x},\bar{p})$ is symplectic and, repeated n times for each of different initial conditions; it can be used to make judgment on beam stability. The rough estimate of the area of beam stability can be obtained from the matrix M describing the transformation of an infinitesimal vector $(\Delta x,\ \Delta p)$. The trace of the matrix is given by

$$\frac{Tr(M)}{2} = \cos\phi + (\frac{3\lambda}{2\omega})(x')^2\sin\phi. \tag{3}$$

The beam is unstable if $\frac{Tr(M)}{2} > 1$. We choose parameters $\lambda/\omega = 0.1$, $\nu = \phi/(2\pi) = \sqrt{3} - 1$. In this case, the beam is unstable for $|x| > 2.44$.

Periodic perturbation generates series of resonances. In the lowest order, resonances generated by n_0-th harmonics of perturbation can be analyzed by canonical transformation to a resonance-basis Hamiltonian. In the angle-action variables $x = \sqrt{2J/\omega}\sin(\psi + \pi n_0 t/2T)$, $\omega J = p^2/2 + \omega^2 x^2/2$, the resonance-basis Hamiltonian given by

$$H(J\psi) = -\Delta J + \frac{3\Lambda}{2}J^2 + \frac{\Lambda J^2}{2}\cos 4\psi, \tag{4}$$

where $\Delta = (2\pi/T)(n_0 - \nu)$ and $\Lambda = \lambda/(8\pi\omega)$. The motion is limited to the phase space between two parabolas Eq.(4) with $\cos\psi = -1$ and $\cos\psi = 1$. For $\Delta > 0$, fixed points are at $J_r = \Delta/4\Lambda$, $\cos\psi = -1$ corresponding to the minimum energy $H_{min} = -\Delta^2/(4\Lambda)$. The closest fixed points are generated with the chosen parameters by the mode $n_0 = 3$, $x_{FP} = 1.501$. For energy in the interval $-\Delta^2/(4\Lambda) < H < -\Delta^2/(8\Lambda)$, there are two families of trajectories: one around the origin $x = p = 0$, and another one around fixed points. For larger H, only one family survives. The phase space of the classical map given by Eqations (1) and (2) is shown in Fig. 1. The area of the phase space around the hyperbolic fixed point $x = 0$, $p = -1.5$ is zoomed in Fig. 2.

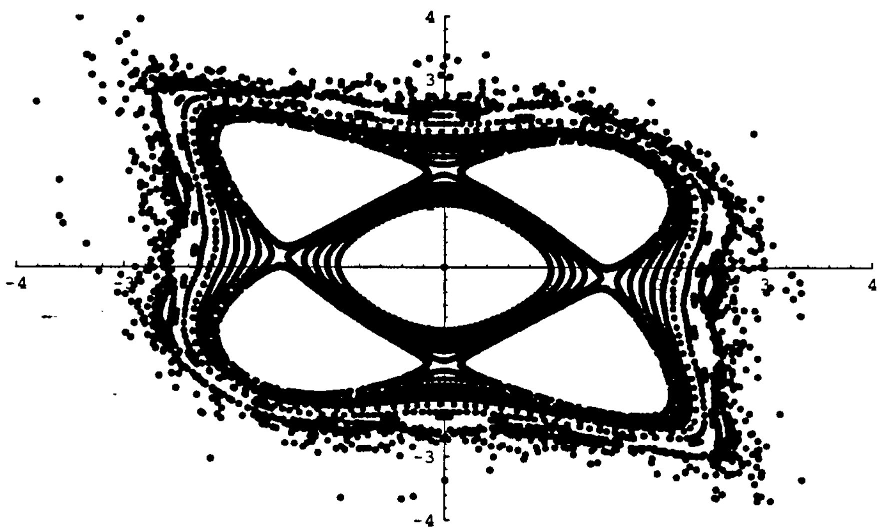

Figure 1: Tracking with a classical map. 1000 turns, 21 particle, $\nu = \sqrt{3} - 1$, $\lambda/\omega = 0.1$.

Generally, a given perturbation generates an infinite number of higher order resonances with a separatrix for each of them. The size of n-th order separatrix caused by perturbation λ is of the order of λ^{2n} and small, but n may be arbitrarily large. The phase space of a classical map has, therefore, a very complicated structure where fixed points of higher order resonances are interleaved with stochastic layers separating them. In quantum mechanics the situation must be quite different. Indeed, the uncertainty principal gives the lowest limit for the size of a separatrix, and sets the limit for the highest possible order of nonlinear resonances driven by perturbation.

The question arises on the limits of applicability of the classical map. One can expect that quantum corrections are small within separatrices where classical motion is stable. Indeed, the centroid of a wave packet should move, in this

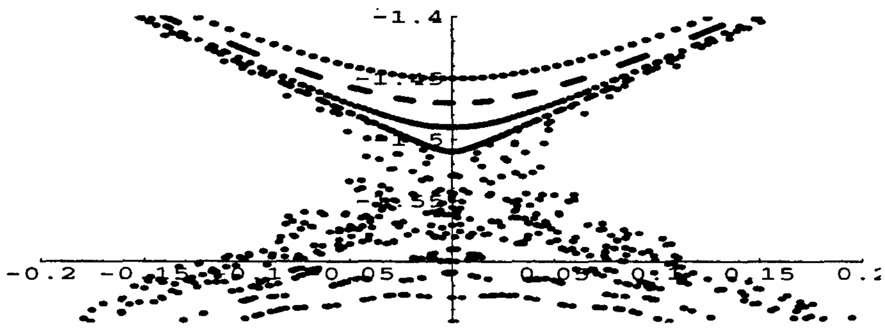

Figure 2: Stochastic trajectories of the classical map.

area, along a classical trajectory, while rms would oscillate with a frequency close to 2ω. The situation may be quite different in stochastic layers. As it is well known, the rms of a wave packet describing a free particle increases in time what corresponds to the linear divergence of classical trajectories in this case. In stochastic layers classical trajectories diverge exponentially. Hence, we can expect that rms of the wave packet would grow in time in a similar fashion. Classical trajectory would be completely meaningless, and the wave function spreads uniformly within stochastic layers along the separatrix boundary. In classical mechanics this statement corresponds to ergodic behavior of trajectory.

This note illustrates the difference of classical and quantum tracking.

2 Quantum Map

The quantum mechanical analog of a classical quantity $F_c(x_c(t), p_c(t))$ is the mean value $F_q =< \psi|F(x,p)|\psi >$. Within separatrices, the operator $F(x,p)$ can be expanded around classical trajectories

$$F_q = F_c(x_c(t), p_c(t)) + (1/2)[\frac{\delta^2 F_c}{\delta^2 x_c}\sigma^2 + \frac{\delta^2 F_c}{\delta^2 p_c}\Delta^2 + 2\frac{\delta^2 F_c}{\delta x_c \delta p_c}\kappa^2] + ... \quad (5)$$

where

$$\sigma^2 =< \psi|(x - x_c)^2|\psi >,$$

$$\Delta^2 = < \psi|(p - p_c)^2|\psi >,$$
$$\kappa^2 = < \psi|(x - x_c)(p - p_c)|\psi > . \tag{6}$$

The quantum mechanical analog of a classical map, therefore, includes the transformation of the rms. It can be obtained from the one-turn transformation of the wave function [1]. The linear transformation corresponding to the Hamiltonian H_0 is given simply as $\varphi = e^{iH_0t/h}\psi$. The wave function φ satisfies the equation

$$ih\delta\varphi/dt = e^{iH_0t/h}V(x,t)e^{-iH_0t/h}\varphi = V(x',t)\varphi. \tag{7}$$

Here $V(x',t)$ is obtained from $V(x,t)$ by replacing operator x with

$$x' = e^{iH_0t/h}xe^{-iH_0t/h} = x\cos\phi + (p/\omega)\sin\phi, \phi = \omega t.$$

Note, that the linear transformation of the operators x, p is identical to that of classical coordinates in Eq. (1). The kick in the RHS of Eq. (5) changes φ to $\bar{\varphi} = e^{-iV_0(x')/h}\varphi$. Hence, the wave function is transformed as

$$\begin{aligned}\psi(x,n+1) &= e^{iH_0(n+1)T/h}e^{-iV_0(x')/h}e^{-iH_0nT/h}\psi(x,n) \\ &= e^{-iV_0(x)/h}e^{-iH_0T/h}\psi(x,n).\end{aligned} \tag{8}$$

The average $F_q(n+1) = < \psi(n+1)|F(x,p)|\psi(n+1) >$ is

$$F_q(n+1) = < \psi(n)|e^{iH_0T/h}e^{iV_0(x)/h}F(x,p)e^{-iV_0(x)/h}e^{-iH_0T/h}|\psi(n) >$$

or

$$\begin{aligned}F_q(n+1) &= < \psi(n)|e^{iH_0T/h}\sum_{m=0}^{\infty}\frac{(i/h)^m}{m!}[V_0(x)[V_0...[V_0, F(x,p)]]]e^{-iH_0T/h}|\psi(n) > \\ &= \sum_{m=0}^{\infty}\frac{(i/h)^m}{m!} < \psi(n)|[[V_0(x',p'),...[V_0(x',p'), F(x',p')]]|\psi(n) >,\end{aligned} \tag{9}$$

where the operators, (x', p'), are given in terms of the operators x, p by Eq. (1) with a one-turn phase advance $\phi = \omega T$.

Considering quadrupole kick, we may redefine the Hamiltonian $H_0 = p^2/2 + \omega^2x^2/2$ by adding and subtracting the linear term $\alpha x^2/2$ to suppress secular terms. Eq. (7) gives the following map for the mean value quantities:

$$
\begin{aligned}
x(n+1) &= x', \\
p(n+1)/\omega &= p'/\omega - (\lambda/\omega)x'^3 - (\lambda/\omega)\, x'[3(\sigma^2)' - \alpha]; \\
\sigma^2(n+1) &= (\sigma^2)'; \\
\kappa^2(n+1) &= (\kappa^2)' - 2(\lambda/\omega)(\sigma^2)'[3x'^2 - \alpha] - 6(\lambda/\omega)((\sigma^2)')^2; \\
\Delta^2(n+1) &= (\Delta^2)' - (\lambda/\omega)(\kappa^2)'[3x'^2 - \alpha] + (\lambda/\omega)^2[x'^2(x'^2 - \alpha)^2 \\
&\quad + (\sigma^2)'(3x'^2 - \alpha)^2 + 6(\sigma^2)'x'^2(x'^2 - \alpha) - x'^2(3\sigma'^2 - \alpha)^2 \\
&\quad - 2x'^4(3\sigma'^2 - \alpha) - x'^6] - 3(\lambda/\omega)(\sigma^2)'(\kappa^2)' \\
&\quad + 3(\lambda/\omega)^2[(\sigma^2)']^2(15x'^2 - 2\alpha) + 15(\lambda/\omega)^2[(\sigma^2)']^3. \qquad (10)
\end{aligned}
$$

Rotation by the angle $\phi = \omega T$ is given by the following

$$
\begin{aligned}
x' &= x(n)\cos\phi + (p(n)/\omega)\sin\phi; \\
p'/\omega &= -x(n)\sin\phi + (p(n)/\omega)\cos\phi, \\
(\sigma^2)' &= \sigma^2(n)\cos^2\phi + \Delta^2(n)\sin^2\phi + (1/2)\kappa^2(n)\sin 2\phi; \\
(\Delta^2)' &= \Delta^2(n)\cos^2\phi + \sigma^2(n)\sin^2\phi - (1/2)\kappa^2(n)\sin 2\phi; \\
(\kappa^2)' &= -\sigma^2(n)\sin 2\phi + \Delta^2(n)\sin 2\phi + \kappa^2(n)\cos 2\phi \qquad (11)
\end{aligned}
$$

To derive these formulas, we used Eq. (7) and, to close the system of equations, represented the higher order mean values as

$$
< \psi(n)|(x - x_c)^{2n}|\psi(n) >= \frac{(2n)!}{2^n n!}[< \psi(n)|(x - x_c)^2|\psi(n) >]^n. \qquad (12)
$$

The arguments for this approximation are different depending on whether the classical trajectory is within a separatrix or it is in the stochastic layers. In the separatrix, the motion is stable and, if the wave packet is initially narrow, it remains narrow in time. Corrections given by the first order rms terms should be sufficient. In this case, the map given by Eq. (8) can be simplified by neglecting the term proportional to $((\sigma^2)')^2$ in the expression for $\kappa^2(n+1)$ and all terms in the two last lines in the equation for $\Delta^2(n+1)$.

Classical motion within stochastic layers is random, and, therefore, we can expect that higher-order correlators decay with time faster than the lower-order correlators and can be neglected. In this case, everything can be expressed in terms of the lower-order rms as shown in Eq. (10). Eqs. (8)

and (9) are the quantum map. Initial conditions $x(0) = x_0; p(0) = p_0$ are equivalent to classical trajectory which starts from (x_0, p_0) at $t = 0$. The rms $\sigma^2(0), \Delta^2(0)$, and $\kappa^2(0)$ are arbitrary but limited by the uncertainty principal $\sigma^2(0)\Delta^2(0) > (\hbar/2)^2$. Note that it is the only place where the Planck's constant enters into consideration. Apart from this limitation, Eqs. (8) and (9) can be also considered as a classical map for a narrow distribution function.

The quantum map given by Eqs. (8) and (9) describes the transformation of five variables contrary to the classical map given by Eqs. (1) and (2) for only two variables. To our understanding, the notion of symplecticity can not be applied here. The reason for this can be quite fundamental: the quantum map given by Eqs. (8) and (9) describes the transformation of a coarse-grain distribution function. It is well known, that such a function satisfies the Fokker-Planck equation and so irreversible in time and, therefore, its transformation can not be symplectic.

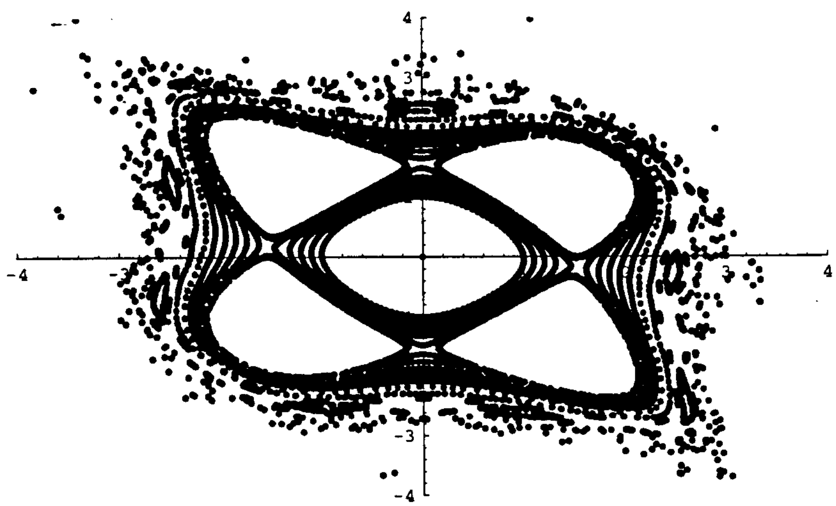

Figure 3: Tracking with "quantum" map. All parameters are identical to Fig. 1.

3 Quantum Tracking

Results of tracking with the quantum map Eqs. (8) and (9) are shown in Fig. 3, and, with zooming, in Fig. 4. The same initial conditions for coordinates are used here as were used above for the classical map. Initial conditions for rms $\sigma^2(0) = \Delta^2(0) = 10^{-15}$, and $\kappa^2(0) = 0$ were chosen.

We compared full quantum tracking with tracking with the simplified map where we neglected terms proportional to the second and third order rms terms. The difference is quite visible for trajectories close to the separatrix although the neglected terms are less than 10^{-30}. On the other hand, we did not notice any difference tracking for few thousand turns with $\alpha = 0$ and $\alpha = 3\sigma^2(0)$ needed to cancel secular terms.

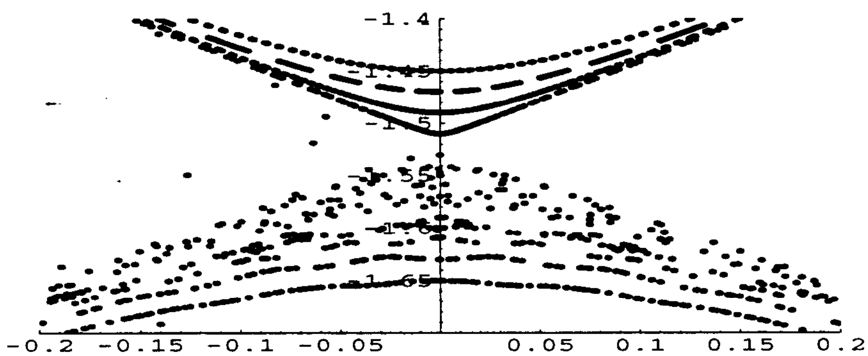

Figure 4: The same as in Fig. 3 with zooming

The overall results are similar to those of the classical map as shown in Fig. 1 and Fig. 2. Identical parameters (tune, λ, number of particles and turns) were used in classical and quantum tracking. Trajectories corresponding to stable motion are practically identical in both cases. There is, however, an important difference: a gap within stochastic layer is noticeable comparing Fig. 2 and Fig. 4. Fig. 5 and Fig. 6 give zooming of the same area close to the hyperbolic point. The same difference can be noticed: the quantum map tends to suppress stochastic motion as could be expected.

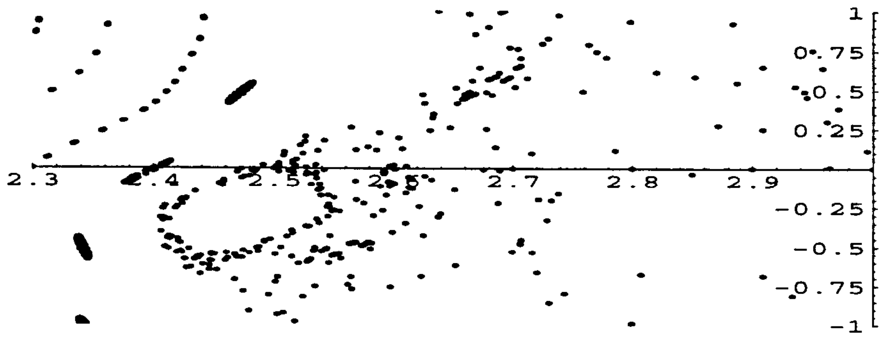

Figure 5: Zooming of the classical map.

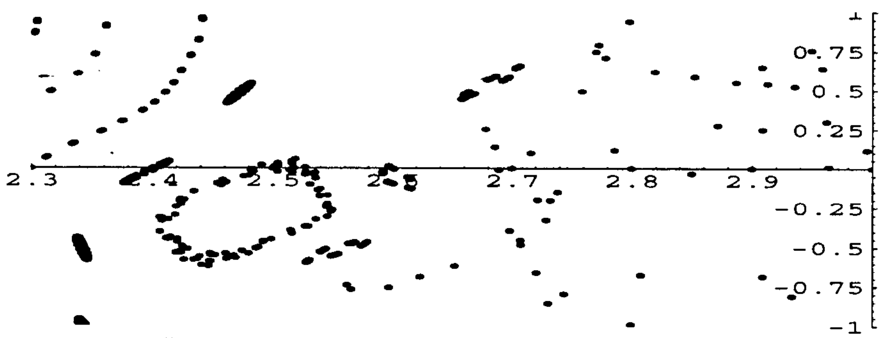

Figure 6: The same area for the quantum map.

4 Conclusion

In this note we give a simple example of the quantum effect in tracking. We confirmed expectations based on physical arguments that quantum corrections can substantially affect the classical results of tracking for trajectories close to the separatrix. Results show that trajectories close to the separatrix are strongly perturbed in spite of the very small initial rms (10^{-15}) and small (1500) number of turns. Furthermore, quantum tracking shows rms is very sensitive to the distance from the separatrix. Hence, the quantum map can be useful in fast findings of the boundaries of nonlinear resonances.

The "quantum" map derived here does not contain Planck's constant explicitly and can be as well considered as a map describing transformation of momenta of classical distribution function. Planck's constant enters only in initial conditions for rms, setting a lowest limit consistent with the uncertainty principle. From this point of view, the quantum map is equivalent to the map for coarse-grain distribution function.

Acknowledgments

We thank Pisin Chen for encouragement.

References

[1] G. Casati, B.V. Chirikov, F.M. Israilev, G. Ford, "Stochastic Behavior of a Quantum Pendulum under a Periodic Perturbation." INP, Novosibirsk (1978).